Subunit Interactions Provide a Significant Contribution to the Stability of the Dimeric Four-α-Helical-Bundle Protein ROP†

Christian Steif, Peter Weber, and Hans-Jürgen Hinz*

Institut für Physikalische Chemie der Westfälischen Wilhelms-Universität, Schlossplatz 4/7, 4400 Münster, Germany

Josef Flossdorf

Gesellschaft für Biotechnologische Forschung mbH, MISF Mascheroder Weg 1, 3300 Braunschweig, Germany

Gianni Cesareni

Dipartimento di Biologica, II Università di Roma, Torvergata Roma, Italy

Mike Kokkinidis

Institute of Molecular Biology & Biotechnology, P.O. Box 1527, Heraklion 71110, Crete, Greece

Received August 10, 1992; Revised Manuscript Received December 15, 1992

ABSTRACT: Detailed thermodynamic and spectroscopic studies were carried out on the ColE1-ROP protein in order to establish a quantitative basis for the contribution of noncovalent interactions to the stability of four-helix-bundle proteins. The energetics of both heat- and GdnHCl-induced denaturation were measured by differential scanning microcalorimetry (DSC) and/or by following the change in circular dichroism in the far-UV range. Sedimentation equilibrium analyses were performed to characterize the state of aggregation of the protein. No intermediate species could be detected during thermal unfolding of the dimer in the absence of GdnHCl. Under these conditions ROP unfolding exhibits a strict two-state behavior. The thermodynamic parameters for the reaction $N_2 \Leftrightarrow 2D$ are $\Delta H_D = 580 \pm 20$ kJ·(mol of dimer)$^{-1}$, $\Delta C_p = 10.3 \pm 1.3$ kJ·(mol of dimer)$^{-1}$·K^{-1}, and $T_m = 71.0 \pm 0.5$ °C. The corresponding Gibbs energy change of unfolding is $\Delta G_D° = 71.7$ kJ·(mol of dimer)$^{-1}$ at 25 °C and pH 6. In the presence of 2.5 M GdnHCl, however, ROP dissociates into monomers at elevated temperatures, as the loss of the concentration dependence of T_m and the decreased molecular weight demonstrate. The corresponding transition parameters are ΔH_D (2.5 M GdnHCl) = 130 ± 10 kJ·(mol of monomer)$^{-1}$ and $T_m = 51.6 \pm 0.3$ °C. Isothermal unfolding studies at 19 °C using GdnHCl as denaturant yielded a Gibbs energy change of unfolding of 22.4 kJ·(mol of monomer)$^{-1}$. This extrapolated value is 38% lower than the corresponding $\Delta G_D°$ value of 35.85 kJ·(mol of monomer)$^{-1}$ calculated from thermal unfolding for the monomer in the absence of GdnHCl, where the protein is known to be a dimer. These results suggest that subunit interactions are an important source of stabilization of the native four-helix-bundle structure of ROP.

A frequently occurring structural motif in proteins is the four-helix-bundle structure (Weber & Salemme, 1980; Cohen & Parry, 1986, 1990). It is characterized by a periodic disposition of apolar residues at positions *a* and *d* within a heptad repeat of the form $(abcdefg)_n$ (Figures 1 and 2). This type of periodicity is not only common in fibrous proteins but also characteristic of most membrane proteins and is found as well in a wide range of globular proteins. Optimal packing interactions occur when the axes of the right-handed α-helices are slightly deformed into a left-handed supercoil (Crick, 1953).

A variety of functionally different proteins such as myohemerythrin, tobacco mosaic virus coat protein, cytochrome *c'*, and apoferritin display the four-α-helix-bundle structure. A very pure realization of this structural motif is found in ColE1-ROP[1] protein, which is a homodimeric four-helix-bundle protein with a molecular mass of 14 kDa (Figure 1). ROP is involved in the regulation of replication of ColE1 and related plasmids in *Escherichia coli* (Twigg & Sherrat, 1980, Cesareni et al., 1982; Tomizawa & Som, 1984; Tomizawa, 1990; Cesareni et al., 1991). It is the product of the *rop* gene and exerts its control function by enhancing the rate of complex formation between two regulatory RNA molecules, RNA I and RNA II (Tomizawa, 1990).

The three-dimensional structure is known from X-ray crystallography to a resolution of 1.7 Å (Banner et al., 1987). Recent two-dimensional NMR analysis corroborates the structure in solution (Eberle et al., 1990). Each of the two ROP monomers has an exact dyad perpendicular to its long axis. ROP was the first coiled-coil structure to be solved at high resolution. Each monomer consists of two antiparallel

† H.-J.H. greatfully acknowledges support from the Deutsche Forschungsgemeinschaft and from the European Community BRIDGE project. The work done in the laboratory of G.C. was also supported by "Progetto Finalizzato Biotecnologie e Biostrumentazione" and by "Progetto Finalizzato Ingegneria Genetica" of CNR.

* Author to whom correspondence should be addressed.

[1] Abbreviations: GdnHCl, guanidine hydrochloride; EDTA, ethylenediaminetetraacetic acid; DTT, dithiothreitol; SDS–PAGE, sodium dodecyl sulfate–polyacrylamide gel electrophoresis; CD, circular dichroism; PMSF, phenylmethanesulfonyl fluoride; NMR, nuclear magnetic resonance; DSC, differential scanning calorimetry; ROP *r*epressor *o*f *p*rimer (equivalent name: ROM, *R*NA *o*ne *m*odulator); ΔH_{vH}, van't Hoff enthalpy; ΔH_{cal}, calorimetric enthalpy obtained from the area under the excess C_p curve.

0006-2960/93/0432-3867$04.00/0

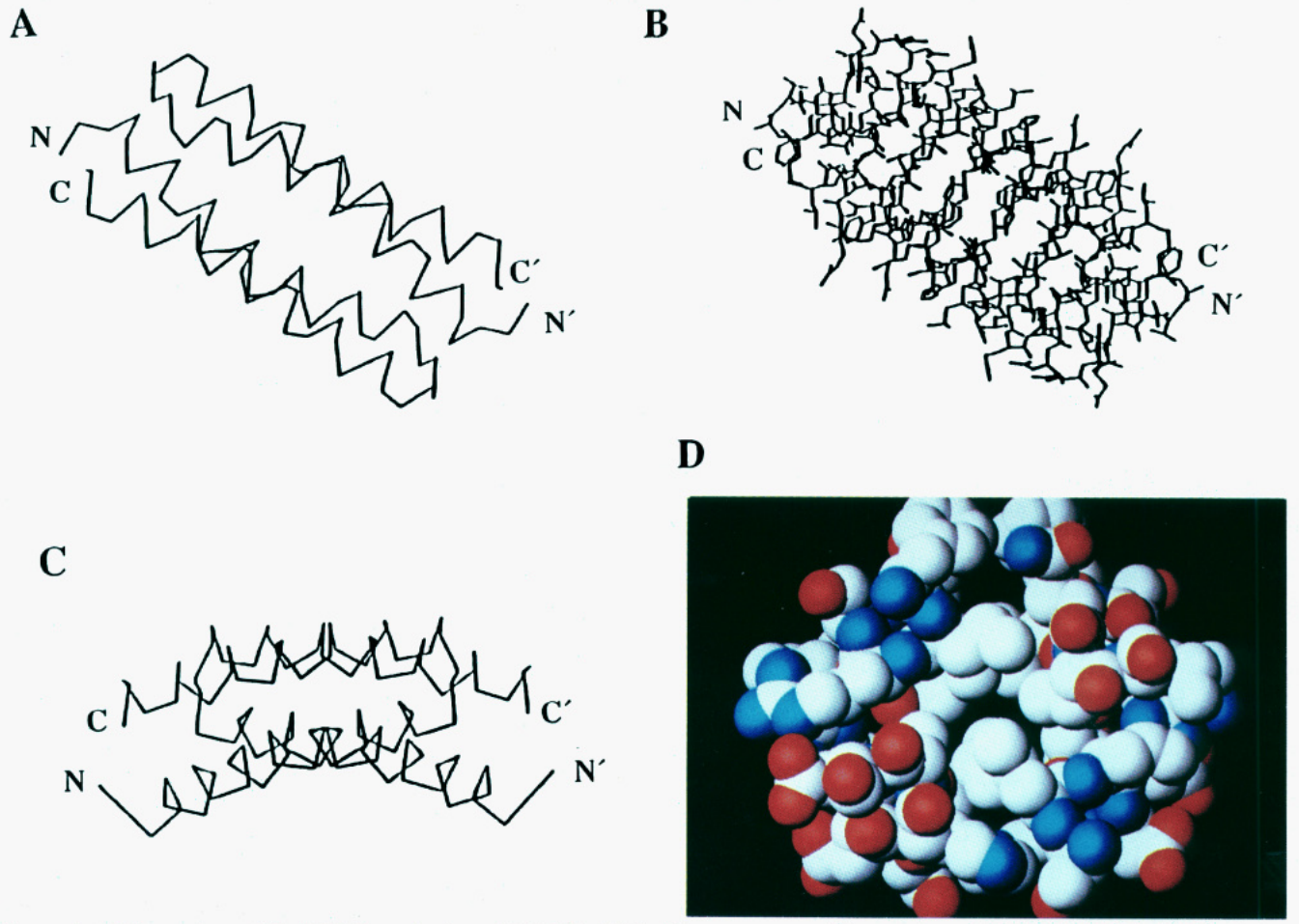

FIGURE 1: Different views of the ROP dimer (amino acids 1–56): (A) backbone structure; (B) same view as in (A) with amino acid side chains shown to illustrate interdigitation of core residues; (C) 90° rotation along the *x*-axis of the structure in (A) to demonstrate curvature of the four-helix bundle; (D) cross-sectional view of the ROP dimer at amino acids Arg13/Thr21 and Glu39/Glu47.

α-helices of approximately the same length, connected by a short linker segment. Interestingly, the last seven amino acids of the C-terminal end cannot be located in the X-ray structure, probably due to high flexibility of these residues.

Our interest in ROP stems from the fact that it appears to be an ideal natural model system for elucidating thermodynamic and kinetic folding parameters of four-helix-bundle structures. The criteria on which we base this choice are the existence of high-resolution X-ray data (Banner et al., 1987) and the availability of a large variety of strategically mutated proteins (Castagnoli et al., 1989).

In this thermodynamic study we report the characteristic transition parameters of wild-type ROP protein. The eminent feature of native ROP protein is its relatively high specific stability of $\Delta g = 5.0$ J·g^{-1} that results to a large extent from the contribution of intersubunit interactions. The unfolding sequence $N_2 \Leftrightarrow 2N^* \Leftrightarrow 2D$ applies to thermal and denaturant unfolding. However, in thermal denaturation a vanishing percentage of native-like monomeric intermediates, N*, occurs, whereas in the presence of 2.5 M GdnHCl the native-like monomer appears to be preferentially stabilized over the dimer at elevated temperature.

MATERIALS AND METHODS

Experiments were carried out in 10 mM sodium phosphate buffer containing 10 mM Na_2SO_4 and 1 mM EDTA, unless otherwise indicated. GdnHCl, ultra pure, was purchased from Schwarz/Mann (Cleveland, OH). Quartz-bidistilled water was used throughout. Protein concentrations refer to the molar mass of the monomeric protein (MW = 7228 g mol^{-1}).

Protein Purification. ColE1-ROP protein was prepared according to the procedure described by Lacatena et al. (1984) with minor modifications. One hundred grams of frozen cells (−80 °C) were suspended in 200 mL of buffer A (50 mM Tris, 0.15 M NaCl, 0.5 mM DTT, 1 mM EDTA, and 0.05% NaN_3, pH 8.5). DNase I and $MgSO_4$ were added to a concentration of 1 mM, and the suspension was then passed twice through a French-press cell (Aminco, Slim Instruments Inc.). PMSF (final concentration of 1 mM) was given to the broken cells to inhibit proteolysis. Cell debris was separated by centrifugation in an SS-34 rotor at 15 000 rpm for 0.5 h. The pellet was resuspended in buffer A and again centrifuged. The supernatant was then ultracentrifuged in an RP-42 rotor at 42 000 rpm for 2 h. The supernatant was loaded onto a DEAE-Sephacel column that had previously been equilibrated with buffer A, omitting NaCl. Protein was eluted with a linear NaCl gradient (0.15–0.6 M NaCl) in buffer A. ROP-containing fractions were monitored using SDS–PAGE, pooled, and concentrated to a final volume of 5 mL. The concentrated fractions were separated from higher molecular weight species by size-exclusion chromatography on an AcA 54–Ultrogel column. Finally, ROP was further purified by employing a hydroxyapatite–Ultrogel column and stored frozen in small aliquots at −20 °C. No contaminants could be detected by SDS–PAGE in the final product.

Protein concentration was determined by absorbance at 280 nm using an extinction coefficient of 0.24 cm^2·mg^{-1}. This

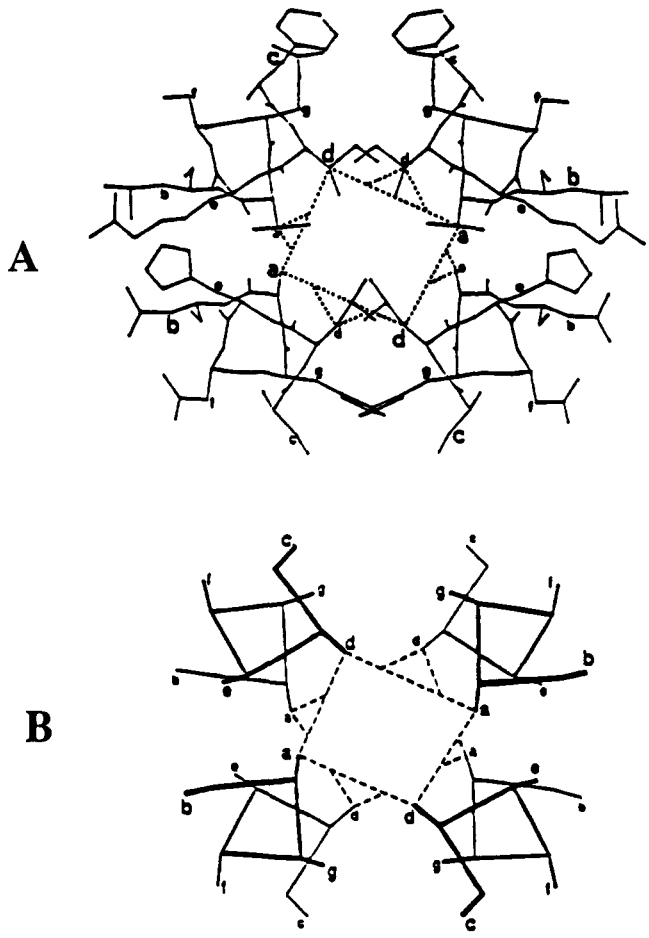

FIGURE 2: Idealized representation of a slice of the ROP four-stranded rope. A detailed description of the preferential occupation of positions *a–g* by specific residues can be found in Banner et al. (1987).

value is based on the amino acid composition and was calculated according to Perkins (1986). Concentration of GdnHCl was determined from the refractive index as described by Nozaki (1972). For the DSC experiments GdnHCl solutions were passed through 0.22-μm Millipore filter membranes.

Differential Scanning Calorimetry. All DSC scans were performed with electronically modified Privalov-type DASM 1 or DASM 4 microcalorimeters (Privalov et al., 1975) having cell volumes of 1 and 0.474 mL, respectively. Heat capacity and temperature data were routinely taken every 0.1 K using a Keithley DMM 192 voltmeter and were stored on a personal computer. Calculation of C_p values was done using a value of 0.72 mL·g^{-1} for the partial volume ($\bar{v}$) of the sample. Typical protein concentrations for the calorimetric experiments were between 0.5 and 1.0 mg·mL^{-1}. Each sample run was preceded by a base-line run with buffer-filled cells. Electrical calibration of the instruments was performed using 50-μW power signals. Integration of the transition curves was done numerically. Unless indicated otherwise, ΔH_{vH} values were calculated according to the van't Hoff equation for a bimolecular process (Marky & Breslauer, 1987):

$$\Delta H_{vH} = 6RT_m^2 \frac{C_{p,max}}{\Delta H_{cal}} \quad (1)$$

where T_m represents the midpoint of the unfolding reaction; $C_{p,max}$, the maximal molar excess heat capacity at T_m; and ΔH_{cal}, the molar enthalpy resulting from integration of the area under the transition peak. R is the gas constant (R = 8.3144 J·mol^{-1}·K^{-1}).

Curve Analysis. Simulation of excess enthalpy, H_{ex}, versus temperature curves was done in a similar way to that previously described by Brandts and Lin (1990). For a two-state process, the variation with temperature of the excess enthalpy, H_{ex}, is given by the equation

$$H_{ex} = \frac{[D]}{C_t}(\Delta H(T_m) + \Delta C_p(T - T_m)) \quad (2)$$

[D] is the concentration of the denatured species, and C_t is the total molar protein concentration referred to the molar mass of the monomer. ΔC_p represents the difference in the apparent molar heat capacity between the native and denatured states. [D] as a function of temperature is given by eqs 3 and 4:

$$[D] = \frac{K(T)}{4}\left[-1 + \left(1 + \frac{8C_t}{K(T)}\right)^{1/2}\right] \quad (3)$$

$$K(T) = C_t \exp\left(-\frac{\Delta H(T_m)}{R}\left(\frac{1}{T} - \frac{1}{T_m}\right) + \frac{\Delta C_p}{R}\left(\ln\frac{T}{T_m} + \frac{T_m}{T} - 1\right)\right) \quad (4)$$

Equations 2–4 are based on the dimer–monomer equilibrium $N_2 \Leftrightarrow 2D$, with T_m being the midpoint temperature of the transition, assuming simultaneous dissociation and unfolding. The equilibrium constant is given by the equation $K = 2\alpha^2 C_t/(1 - \alpha)$, where α refers to the degree of unfolding, and C_t is the total protein concentration in terms of monomers ($K(T_m) = C_t$ at $\alpha = 0.5$).

Circular Dichroism. CD measurements were carried out with a JASCO J 500A spectropolarimeter. Unless stated otherwise, spectra were averaged over eight scans and corrected for the buffer signal by means of a JASCO DP 500N data processor. Various CD cuvettes with optical paths lengths ranging from 0.01 to 1 cm were used to cover a wide range of protein concentrations. For measurements below 200 nm, all buffers were degassed, and the sample compartment of the instrument was thoroughly purged with a constant flow of purified nitrogen.

The instrument was calibrated with *d*-(+)-camphorsulfonic acid that had been twice recrystallized from glacial acetic acid. A value of 188 mdeg was used for the ellipticity at 290 nm, employing a 0.6 mg·mL^{-1} solution in a 1-cm cuvette (Yang et al., 1986; Schmid, 1989). Temperature scans were carried out at 222 nm, unless indicated otherwise. A programmable Haake F3 cryothermostat was used for temperature scans and was routinely operated at a scan rate of 1 K·min^{-1} unless indicated otherwise. Temperature was constantly monitored with a thermistor probe in the cell.

Sedimentation Equilibrium Studies. Ultracentrifugation work was performed in a Beckman Model E analytical ultracentrifuge, equipped with electronic speed and RTIC temperature controls, a photoelectric UV scanner, a multiplexer, a monochromator, and a high-pressure light source. The collimating optics had been improved by a novel illuminating system (Flossdorf & Schillig, 1979; Flossdorf, 1980) that enhances the intensity of the rotor illumination by a factor of about 45. The ROP samples were prepared from a concentrated protein stock solution, from a buffer containing 10 mM sodium phosphate, pH 6.0, 10 mM Na_2SO_4, and 1 mM EDTA, and from a 6.5 M GdnHCl stock solution. Each 150-μL sample was run to equilibrium in 12-mm charcoal-

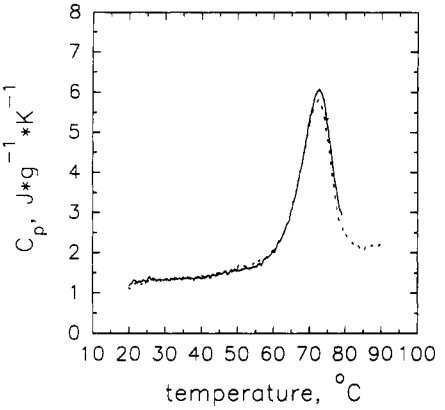

FIGURE 3: Reversibility test: two successive DSC scans with the same sample (1.00 mg·mL^{-1} ROP in 10 mM sodium phosphate, 10 mM Na_2SO_4, and 1 mM EDTA, pH 6). Solid line, first scan; dotted line, second scan. The second scan was recorded immediately after the instrument had cooled down. Heating rate: 1 K·min^{-1}.

filled Epon double-sector cells with sapphire windows, three or five at a time in either a four-place AN-F or a six-place AN-G rotor. After 20–24 h, scans were made at 280 nm and treated in the usual way by plotting C_{prot} versus r^2 according to the equation

$$M = \frac{2RT}{(1-\bar{v}\rho)\omega^2}\frac{\partial(\ln C_{prot})}{\partial r^2} \quad (5)$$

where M denotes the (weight average) molecular weight of the solute; T, the absolute temperature; ω, the angular rotor speed; C_{prot}, the protein concentration; and r, the radial rotor position. The density of the GdnHCl-free buffer at 25 °C was found to be ρ = 0.99949 g·cm^{-3}; the densities of the GdnHCl-containing solvents at the same temperature were calculated according to Kawahara and Tanford (1966). All densities were corrected to the actual temperature assuming that the thermal expansion coefficient of water would be applicable. The partial specific volume of ROP protein, $\bar{v}$ = 0.722 cm^3·g^{-1}, was calculated from its amino acid composition (Cohn & Edsall, 1943). It was assumed to be independent of temperature and, in particular, independent of the presence of GdnHCl.

RESULTS

Thermodynamics of the Unfolding Reaction. Thermally induced unfolding of ROP is highly reversible. Two successive DSC scans with the same sample are shown in Figure 3. The practical identity of the two transition curves is a good indication of the reversibility of the unfolding process. Variation of the scan rate between 0.1 and 1 K·min^{-1} does not result in a significant shift of the unfolding temperature, T_m. Therefore, it can be assumed that thermal unfolding proceeds as an equilibrium reaction. To quantify protein stability, $\Delta G_D°$, for a dimeric system as a function of temperature, the concentration dependence of the unfolding reaction has to be taken into account. The equilibrium constant, $K = 2\alpha^2 C_t/(1-\alpha)$, with α being the degree of unfolding, is not equal to 1 at T_m (α = 0.5), but is equal to C_t, the total molar protein concentration. Hence, $\Delta G_D°$, the Gibbs energy change of unfolding, equals $-RT_m \ln C_t$ at T_m. To obtain standard Gibbs energy parameters, the following equation has been applied

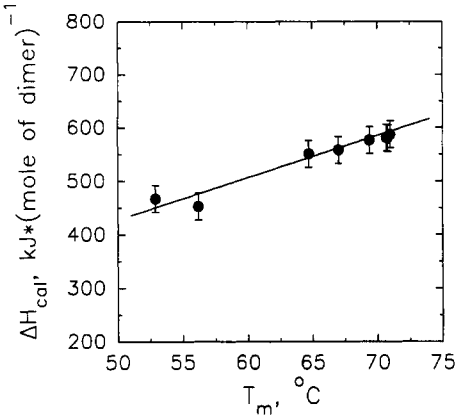

FIGURE 4: Variation with transition temperature, T_m, of the unfolding enthalpy, ΔH_{cal}. The data points reflect the results of DSC scans carried out at different pH values (pH 2–9) with protein concentrations ranging from 0.2 to 1.4 mg·mL^{-1}. Transition temperatures were normalized to a protein concentration of 0.5 mg·mL^{-1}. The solid line represents a linear least squares fitting of the experimental data. The heat capacity change obtained from the slope of the curve is 8 ± 2.5 kJ·(mol of dimer)$^{-1}$·K^{-1}.

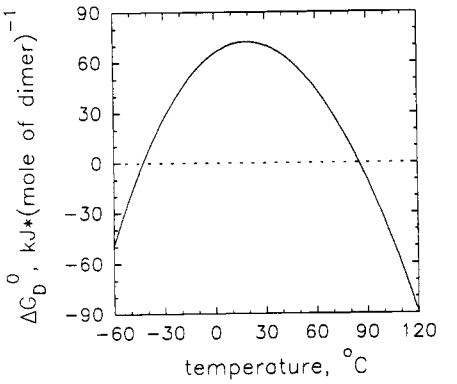

FIGURE 5: Molar standard Gibbs energy change of unfolding, $\Delta G_D°$, of ROP protein as a function of temperature at pH 6.0. $\Delta G_D°$ was calculated according to eq 6 with the parameters given in Table I. The protein concentration was 7 × 10^{-5} M.

to calculate $\Delta G_D°$:

$$\Delta G_D°(T) = \Delta H°(T_m)\left(1-\frac{T}{T_m}\right) + \Delta C_p\left(T - T_m + T\ln\frac{T_m}{T}\right) - RT_m \ln C_t \quad (6)$$

The difference in heat capacity between the native and denatured states has been determined by measuring the unfolding enthalpy as a function of T_m. The unfolding temperature was varied by changing the pH of the solution. ROP has a stable structure over a large range of pH from 1 to 9, as judged from CD spectra in the far-UV region. A strong increase in turbidity indicates precipitation only near the isoelectric point, at about pH 5 (Tomizawa & Som, 1984).

Figure 4 shows the dependence of ΔH_{cal} on the transition temperature, T_m. Linear regression analysis of the data yields a ΔC_p of 8 ± 2.5 kJ·(mol of dimer)$^{-1}$·K^{-1}. Direct ΔC_p determination from the individual transition curves results in moderately larger numbers [ΔC_p = 10.3 ± 1.3 kJ·(mol of dimer)$^{-1}$·K^{-1}].

Figure 5 shows the standard Gibbs energy as a function of temperature for pH 6. The corresponding values for ΔH_{cal}, ΔH_{vH}, $\Delta S°$, T_m, and ΔC_p employed in the calculation are summarized in Table I. The value for the ratio $\Delta H_{vH}/\Delta H_{cal}$ is also included in Table I. Within the limits of error it is

Table I: Thermodynamic Parameters of the Unfolding Reaction of Dimeric ROP Protein in the Presence and Absence of GdnHCl as Derived from DSC Experiments[a]

GdnHCl concn (M)	$\Delta H_{cal}(T_m)$ (kJ·mol^{-1})	$\Delta H_{vH}(T_m)$ (kJ·mol^{-1})	$\Delta S°(T_m)$ (J·mol^{-1} K^{-1})	T_m (°C)	ΔC_p (kJ·mol^{-1} K^{-1})	$\Delta G_D°$ (25 °C) (kJ·mol^{-1})	$\Delta H_v / \Delta H_{cal}$
0	580 ● 20	542 ± 18	1686 ± 58	71.0 ± 0.5	10.3 ± 1.3	71.7	0.935
2.5	260 ± 20[b]	295 ± 42[b]		51.6 ± 0.3	12.7 ± 0.6[b]		

[a] Calorimetric measurements were carried out at pH 6.0 in 10 mM sodium phosphate buffer containing 10 mM Na_2SO_4 and 1 mM EDTA. The scanning rate employed was 1 K·min^{-1}. The $\Delta G_D°$ value was calculated using ΔC_p = 10.3 kJ·(mol of dimer)$^{-1}$·K^{-1}, ΔH_{cal} = 580 kJ·(mol of dimer)$^{-1}$, and T_m = 71 °C (344.15 K). The T_m value refers to a protein concentration of 0.5 mg·mL^{-1}. Each ΔH value is the average of at least six independent measurements, except in the presence of GdnHCl, where only two measurements were performed. The van't Hoff values were calculated with a factor of 4 instead of 6 in eq 1 for measurements performed in the presence of GdnHCl to account for the monomeric state of ROP. [b] In the presence of 2.5 M GdnHCl these thermodynamic parameters must be considered apparent quantities due to the interaction with GdnHCl as discussed.

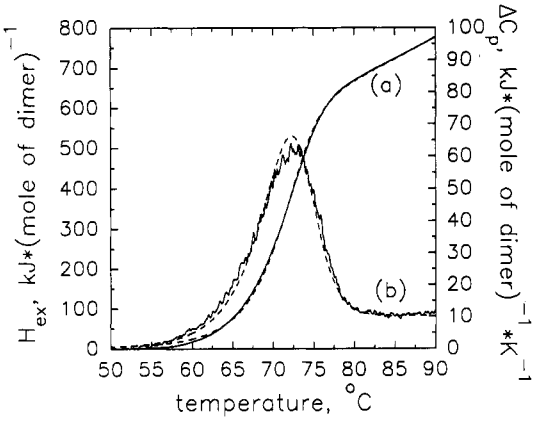

FIGURE 6: Results of the DSC-curve analysis assuming a two-state process as described in the text (solid lines, experimental curves; broken lines, fitted curves). The experimental conditions were 1.0 mg·mL^{-1} ROP in 10 mM sodium phosphate buffer containing 10 mM Na_2SO_4 and 1 mM EDTA, pH 6. (a) The experimental excess transition enthalpy as a function of temperature has been obtained from the calorimetric heat capacity curves by integration employing the linear heat capacity function of the native state as base line. The dashed curve shows the theoretical H_{ex} versus temperature function obtained from nonlinear least squares fitting of the experimental parameters by using eq 2. The optimal parameters resulting from the analysis are $\Delta H°$ = 569 kJ·(mol of dimer)$^{-1}$, T_m = 70.7 °C, and ΔC_p = 10.7 kJ·(mol of dimer)$^{-1}$·K^{-1}. For comparison, the quantities derived directly from the heat capacity curves are ΔH_{cal} = 580 kJ·(mol of dimer)$^{-1}$, T_m = 71 °C, and ΔC_p = 10.3 kJ·(mol of dimer)$^{-1}$·K^{-1}. (b) Comparison of the experimental and theoretical C_p curves. The solid line refers to the experimental measurement, and the dashed line refers to the two-state model of unfolding according to $N_2 \rightleftharpoons 2D$ (eq 3). The C_p curves have been obtained from the corresponding excess enthalpy functions shown in (a) by numerical differentiation.

equal to 1, thus indicating a two-state behavior of the thermal unfolding reaction. The T_m value listed refers to a protein concentration of 7 × 10^{-5} M (≅0.5 mg·mL^{-1}). T_m values for other concentrations can be calculated with use of eq 7, which gives the dependence of the reciprocal transition temperature on the natural logarithm of the protein concentration.

Thermal Unfolding of ROP Follows a Two-State Mechanism. Line-shape analysis of heat capacity transition curves can be used to sort out unfolding mechanism incompatible with the thermodynamic measurements. For practical reasons, we apply the fitting procedures to the integrated excess enthalpy, H_{ex}, versus temperature curves and regenerate the heat capacity versus temperature functions by numerical differentiation. Figure 6a illustrates the quality of such a fit. The H_{ex}/T curve (solid line) has been obtained by integration of the experimental heat capacity function, using the extrapolated linear heat capacity of the native state $C_p^N(t)$ = (2.520 × 10^{-3})t + 1.435 in J·g^{-1}·K^{-1}, where t refers to °C, as a base line. The heat capacity change $\Delta C_p(T_m)$ in the transition peak corresponds to the constant slope of the H_{ex}/T curve at high temperatures. The dashed curve which practically coincides with the experimental enthalpy function is the theoretical H_{ex}/T curve. It has been generated under the assumption of a strict two-state mechanism (eqs 2–4) employing the following parameters: ΔH_{cal} = 569 kJ·(mol of dimer)$^{-1}$, T_m = 70.7 °C, and ΔC_p = 10.7 kJ·(mol of dimer)$^{-1}$·K^{-1}. The good agreement between the experimental and the theoretical curve strongly supports the correctness of the two-state assumption for the thermal unfolding reaction.

GdnHCl-Induced Transitions. The solvent-induced unfolding of ROP was followed by measuring its ellipticity at 222 nm in the presence of increasing concentrations of GdnHCl. Typically, 25 μL of a ROP stock solution (≈2 mg·mL^{-1}) was injected into 475 μL of an appropriate solution of GdnHCl in 10 mM sodium phosphate buffer, pH 6, containing 10 mM Na_2SO_4, 1 mM EDTA, and 1 mM DTT. These samples were incubated for 20 h at 19 °C before CD spectra were recorded.

The corresponding refolding experiments were performed as follows: a stock solution of ROP in 8.3 M GdnHCl was incubated for 20 h at 19 °C. Fifty microliters of this solution was then injected into 450 μL of a GdnHCl solution containing the desired final concentration of the denaturant for the refolding assay. CD spectra were taken after a 24-h refolding incubation at 19 °C. Care was taken to ensure that unfolding and refolding studies were performed using identical final protein concentrations.

Figure 7a shows typical CD spectra of ROP in 0, 2.5, 4.5, and 7.5 M GdnHCl. The very pronounced band with two minima, at 210 and 222 nm, having mean residue ellipticities of about −30 000 deg·cm^2·dmol^{-1} reflects the high degree of α-helicity of the protein. It is noteworthy that spectra at 0 and 2.5 M GdnHCl at a temperature of 19 °C are identical within error limits. This shows that under these low temperature conditions 2.5 M GdnHCl does not yet perturb the structure of ROP. Sedimentation equilibrium studies in the ultracentrifuge demonstrate an unchanged molecular weight that corresponds to that of the dimer. Only at about 4 M GdnHCl does the molecular weight start to decrease at 19 °C, which is also seen in the decreased mean residue ellipticity of the corresponding spectrum in Figure 7a.

Figure 7b exhibits GdnHCl unfolding and refolding experiments at 19 °C using the mean residue ellipticity, [Θ], at 222 nm as probe of α-helix content. The curve with the solid circles refers to unfolding; the curve showing the open circles, to refolding equilibrium. A distinct hysteresis behavior is observed at this temperature, even after an incubation time of 7 days for refolding. Increasing the temperature to 30 °C, however, results in a strong decrease of this kinetic effect, with only a difference of 0.5 M remaining in the value of $c^{50\%}_{GdnHCl}$, the midpoint concentration of the GdnHCl-induced unfolding transition. At higher temperatures refolding no longer involves hysteresis effects. This is indicated by the

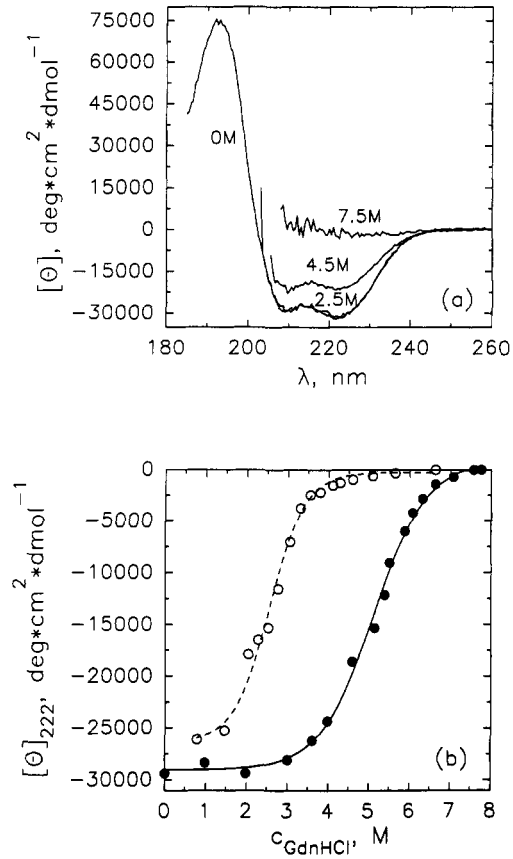

FIGURE 7: (a) CD spectra of native ROP in buffer (10 mM sodium phosphate, 10 mM Na_2SO_4, and 1 mM EDTA, pH 6) and in the same buffer containing 2.5, 4.5, and 7.5 M GdnHCl. The protein concentration was 0.3 mg·mL^{-1}. Mean residue ellipticity of ROP has been plotted as a function of wavelength, using a mean residue weight of 114.7 g·(mol of amino acid)$^{-1}$. (b) GdnHCl-induced denaturation (●) and renaturation (○) curves of ROP at pH 6 and 19 °C. The total protein concentration was 0.1 mg·mL^{-1} in both the unfolding and refolding experiments. The diagram shows the mean residue ellipticity at 222 nm, which was recorded in a 1-mm CD cuvette at a spectral bandwidth of 1 nm. Spectra were averaged over eight scans and buffer corrected against a solution containing 7 M GdnHCl and 1 mM DTT. The lines are spline interpolations of the experimental data.

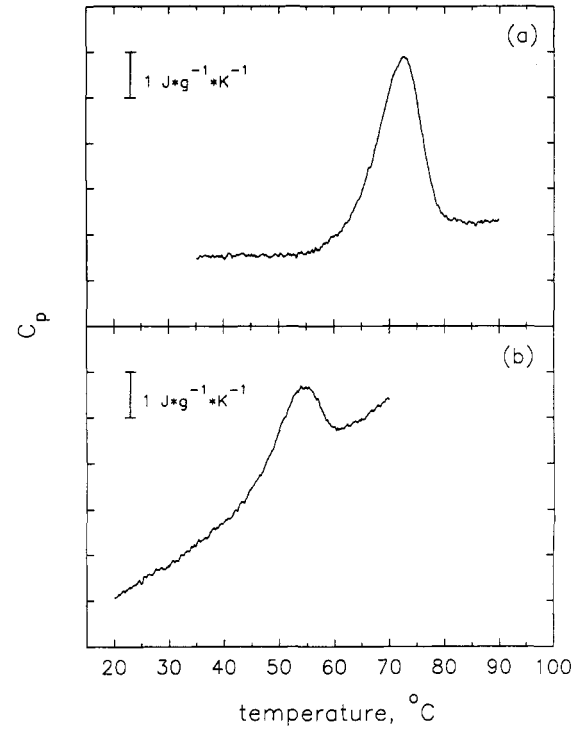

FIGURE 8: DSC scans of ROP in (a) 10 mM sodium phosphate, 10 mM Na_2SO_4, and 1 mM EDTA, pH 6, and (b) 2.8 M GdnHCl. The protein concentration was 0.5 mg·mL^{-1} in both measurements. The heating rate was 1 K·min^{-1}.

complete reversibility of the DSC curves in the presence of GdnHCl (Figure 8b).

At 19 °C the midpoint of the GdnHCl-induced unfolding curve lies at $c^{50\%}_{GdnHCl}$ = 5.3 M. The high concentration of GdnHCl necessary to induce unfolding suggests extraordinary stability of the molecule. The unfolding curve covers a relative broad GdnHCl concentration range, from 3.5 to 6.5 M, which is indicative of a relatively low degree of cooperativity of the unfolding process.

Thermal Denaturation in the Presence of GdnHCl. As pointed out before, no evidence for a significant population of monomeric species is found during the course of thermal unfolding. However, GdnHCl-induced denaturation curves (Figure 7b) exhibit a rather broad transition range suggestive of a lower degree of cooperativity than that obtained from thermal denaturation experiments. To further analyze these apparent differences, we have looked at the influence of GdnHCl on thermal unfolding. DSC scans were performed in the presence of various concentrations of GdnHCl at a protein concentration of 0.5 mg·mL^{-1}. A typical transition curve in the presence of 2.8 M GdnHCl is shown in Figure 8b together with the transition curve of native ROP protein (Figure 8a). With increasing GdnHCl concentrations both the transition temperature and the transition enthalpy, which is proportional to the area under the peak, decrease. Reheating in GdnHCl shows the same degree of reversibility as in the absence of the denaturant. Thus kinetic effects which slow down folding in the low-temperature isothermal experiments play no role at the temperatures of the heat capacity measurements. The results of DSC studies involving nine different GdnHCl concentrations are shown in Figure 9a,b, where both T_m and ΔH_{cal} values are plotted as a function of GdnHCl concentration. Both curves reveal a rather unexpected variation of these thermodynamic parameters with GdnHCl concentration. In the concentration range between 1 and 2 M GdnHCl both the transition temperature, T_m, and the transition enthalpy, ΔH, drop sharply, while between 0 and 0.5 M GdnHCl and above approximately 2.5 M GdnHCl these thermodynamic parameters vary little with the GdnHCl concentration. Above approximately 6.5 M GdnHCl ROP is fully unfolded, and consequently, no transitions involving T_m and ΔH can be observed at these GdnHCl concentrations.

A rationale for the dependence of both T_m and ΔH on the GdnHCl concentration is the following. If one assumes a temperature-dependent change in the state of aggregation of ROP in the presence of 2.5 M GdnHCl, the drop in T_m and ΔH between 0.5 and 2 M GdnHCl seen in Figure 9 can be interpreted as reflecting the difference between the thermodynamic parameters for dimer and monomer unfolding. This interpretation had been suggested by the results of molecular weight determinations in 2.5 M GdnHCl using gel filtration. Clear evidence was provided, however, by the sedimentation equilibrium studies. They showed that in the presence of 2.5 M GdnHCl ROP starts dissociating into monomers around 30–35 °C and is fully monomeric at approximately 50 °C (Figure 10c). Thus the T_m and ΔH values shown in Figure 9a,b essentially reflect two different unfolding mechanisms. At GdnHCl concentrations below 0.5 M the unfolding equilibrium is described by a dimer–monomer reaction, N_2

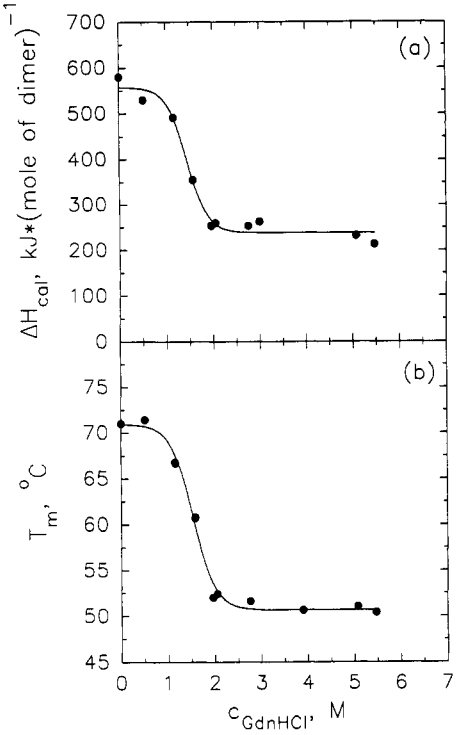

FIGURE 9: (a) Dependence of the transition enthalpy, ΔH_{cal}, on the concentration of GdnHCl at pH 6 derived from DSC measurements. All measurements were run at least in duplicate and were carried out in 10 mM sodium phosphate, 10 mM Na_2SO_4, and 1 mM EDTA, pH 6, in the following GdnHCl concentrations: 0, 0.51, 1.16, 1.57, 1.95, 2.04, 2.76, 3.0, 5.08, and 5.47 M. The protein concentration was 0.5 mg·mL^{-1}. The scanning rate was 1 K·min^{-1}. (b) The corresponding values for the transition temperatures, T_m, as a function of the concentration of GdnHCl for the same experiments as in (a). The solid curves show spline interpolations of the experimental data.

$\Leftrightarrow$ 2D, while at 2.5 M and above the T_m and ΔH values refer to a transition of the type N* $\Leftrightarrow$ D.

To further prove the correctness of this interpretation, we have measured thermal denaturation in the presence of 2.5 M GdnHCl by both CD and DSC in a wide range of protein concentration (0.004–3.3 mg·mL^{-1}).

The rationale is as follows: For an oligomeric system that dissociates upon unfolding, T_m is a function of the total protein concentration. The dependence of T_m on C_t is given by

$$\frac{1}{T_m} = -\frac{R}{\Delta H^\circ} \ln C_t + \frac{\Delta S^\circ}{\Delta H^\circ} \qquad (7)$$

(Hinz, 1979; Marky & Breslauer, 1987) where ΔH° and ΔS° refer to the temperature-independent change in enthalpy and entropy under standard conditions at T_m, respectively. If in the absence of GdnHCl the unfolding of ROP follows preferentially a $N_2 \Leftrightarrow 2D$ mechanism, while in the presence or 2.5 M GdnHCl the prevailing mechanism is N* $\Leftrightarrow$ D, one should expect a variation of the transition temperature, T_m, with protein concentration in the absence of GdnHCl and independence of concentration in the presence of GdnHCl.

The results of a large number of CD and DSC experiments covering a wide range of concentrations (0.004–1.14 mg·mL^{-1}) are given in Figure 10a,b. The significant result is that no concentration dependence of the unfolding temperature can be observed in 2.5 M GdnHCl, whereas the expected variation of T_m with ln C_t occurs in the absence of GdnHCl. This finding clearly demonstrates that in the presence of 2.5 M GdnHCl ROP occurs as a monomer in the vicinity of T_m. An independent proof of the monomeric state of ROP under these

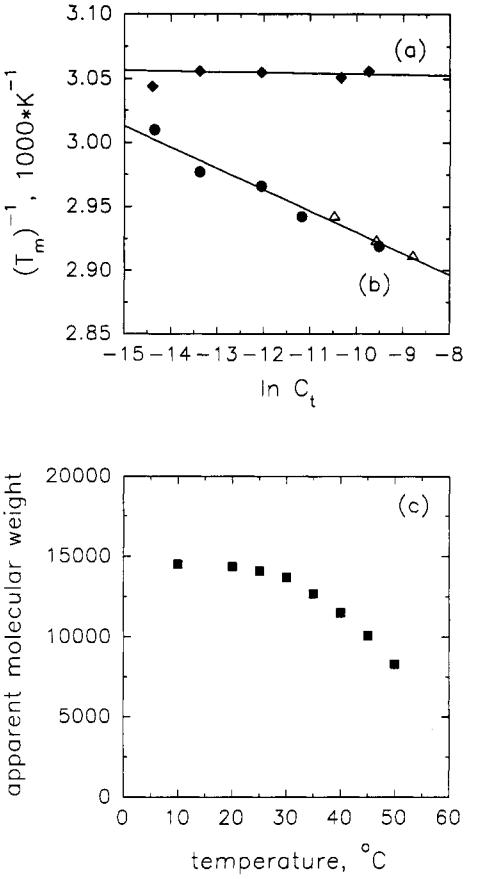

FIGURE 10: Variation of reciprocal unfolding temperature $(T_m)^{-1}$ with the natural logarithm of total protein concentration, C_t, (a) in the presence of 2.5 M GdnHCl and (b) in the absence of GdnHCl. All measurements were carried out in 10 mM sodium phosphate buffer, pH 6, containing 10 mM Na_2SO_4 and 1 mM EDTA. Data taken from DSC scans are marked by open triangles (▲); CD-derived values, by filled dots (●), in the presence of 2.5 M GdnHCl, by filled rhombs (◆). The protein concentration ranged from 0.004 to 1.14 mg·mL^{-1}. The solid lines are the results of linear least squares analyses. (c) Plot of the variation of the apparent molecular weight with temperature in the presence of 2.5 M GdnHCl. Measurements were carried out in 2.5 M GdnHCl in the temperature range from 15 to 55 °C. The ROP samples were run to equilibrium in a four-place AN-F rotor at 22 000–26 000 rpm for more than 24 h.

condition results from the ultracentrifugation studies. Figure 10c shows the molar mass of ROP in the presence of 2.5 M GdnHCl as a function of temperature. The molar mass reaches the value of the monomer at about 50 °C. Equation 7 permits calculation of the transition enthalpy from the slope of the $(T_m)^{-1}$ versus ln C_t curve shown in Figure 10b. The value is ΔH° = 550 ± 20 kJ·(mol of cooperative unit)$^{-1}$. It is in excellent agreement with the ΔH_{cal} value obtained from the direct microcalorimetric studies. The agreement between the van't Hoff enthalpy, ΔH_{vH}, and the calorimetric enthalpy, ΔH_{cal}, is another good indication that the mechanism in the absence of GdnHCl is $N_2 \Leftrightarrow 2D$. A summary of the transition parameters is given in Table I.

DISCUSSION

The present study has been carried out as part of a more general program aimed at investigating the influence of mutations on noncovalent interactions in proteins. ROP has been chosen as model system not only because of its characteristic structural properties as an almost ideal four-α-helix-bundle protein but also because of the availability of

a large number of strategically designed mutants and the progress in X-ray structure analysis of these mutated proteins.

High Specific Stability Can Be Realized by Different Structural Motifs. The present thermodynamic unfolding studies characterize the stability of native ROP (MW = 14 456 g·mol^{-1}) in the biologically interesting temperature range and delineate the unfolding mechanism in the absence and presence of GdnHCl. The Gibbs energy, $\Delta G_D°$ = 71.7 kJ·(mol of dimer)$^{-1}$ = 5.0 J·g^{-1}, is remarkably high compared to other small globular proteins, including those with disulfide cross-links [RNase T1, 4 J·g^{-1} (Kiefhaber et al., 1990); Tendamistat, 3.5 J·g^{-1} (Renner et al., 1992)]. There are some noticeable examples of proteins reported in the literature, however, whose stabilities are of similar or even larger magnitude than those found for ROP (Bellelli et al., 1990). The four-α-helix-bundle-forming peptides [MW = 1880 g·(mol of monomer)$^{-1}$] synthesized in DeGrado's group (Ho & DeGrado, 1987) exhibit free energies of tetramerization on the order of 84 kJ·(mol of tetramer)$^{-1}$ ($\cong$ 11.2 J·g^{-1}). This value can be considered as being representative for the Gibbs energy of unfolding of these synthetic peptides under the assumption that the single peptide lacks any structure in solution. Nojima et al. (1978) reported stabilities of cytochrome *c*-552 (MW = 15 000 g·mol^{-1}) isolated from the hyperthermophilic bacterium *Thermus thermophilus*. The molar Gibbs energy change of this protein is 119 kJ·mol^{-1} at 25 °C, which corresponds to a specific value of 7.9 J·g^{-1}. Another cytochrome *c*-552 (MW = 7600 g·mol^{-1}) from the thermophilic hydrogen-oxidizing bacterium *Hydrogenobacter thermophilus* shows even a much higher stability. The molar and specific Gibbs energy values at 25 °C of this cytochrome are 91.6 kJ·mol^{-1} and 12 J·g^{-1}, respectively. Sequence comparison between this thermophilic protein (Sanbongi et al., 1989) and the mesophilic protein, whose structure is known (Almassy & Dickerson, 1978), suggest that a higher degree of α-helicity may be responsible for the higher thermostability of cytochrome *c*-552.

It is interesting to speculate about an underlying functional or structural principle that may be the cause of this extraordinary stability of these very different proteins. Generally proteins and particularly enzymes of mesophilic organisms are found to be marginally stable (Privalov, 1979; Jaenicke, 1991). Since high specific stability usually also implies rigidity, the relatively low stability of the majority of known enzymes can be rationalized in terms of the necessity for catalytically required flexibility (Huber, 1988). This hypothesis is corroborated by the finding that proteins serving as inhibitors, such as proteinase inhibitors, assume rather stable structures.

The membrane-located cytochromes *c*-552 from thermophilic organisms fit nicely into this picture of functionally determined stability. First, their high resistance to unfolding is essential for maintenance of the native structure at the high temperature of the environment; second, high flexibility inside the membrane may not be required for their function, since their substrates are electrons, whose transfer need not involve large conformational adjustments of the protein (Huber, 1988).

ROP protein serves a biological function that requires mainly correct binding to small flexible RNAs to enhance their rate of complex formation (Tomizawa, 1990). For this reaction proper structure is probably of principal importance, and it can be guaranteed by high specific stability.

GdnHCl Stabilizes Native-Like Monomeric Folding Intermediates. From the present studies it appears to be reasonable to suggest the following unfolding mechanism for ROP:

$$N_2 \Leftrightarrow 2N^* \Leftrightarrow 2D \qquad (8)$$

In the absence of GdnHCl the equilibrium concentration of intermediate monomers, N*, is negligible, as the analysis of the calorimetric transition profiles shows. However, in the presence of 2.5 M GdnHCl we have a different picture. The ultracentrifugation studies clearly demonstrate the occurrence of predominantly monomeric ROP at about 50 °C. CD unfolding curves exhibit under these conditions a T_m value of 51.2 °C independent of protein concentration. The overall change in the mean residue ellipticity is approximately −30 000 deg·cm^2·dmol^{-1} with half of that value remaining at T_m. Thus one has to conclude that the monomers N* retain most of the mean residue ellipticity that they show in the native dimer also after dissociation into the monomeric state. The secondary structure is obviously intact, whereas the tertiary interhelical interactions are perturbed by the presence of GdnHCl, as the strong decreases in T_m and ΔH indicate (Figure 9a,b). We have the intriguing result that 2.5 M GdnHCl promotes dissociation of the dimer and stabilization of the intermediate monomer. Higher concentrations of the denaturant lead to complete unfolding of the residual structure. At first sight this may appear contradictory, but in terms of the thermodynamics of weak binding systems it can be understood qualitatively (Casassa & Eisenberg, 1964; Arakawa et al., 1990; Schellman, 1990; Timasheff, 1992). The basic idea is that principally transfer free energies and preferential interaction parameters may have opposite signs, as convincingly demonstrated by Arakawa et al. (1990) in their studies on β-lactoglobulin. The authors show for this system that preferential interaction can vary strongly and even change sign as a function of denaturant concentration. In view of these results, one can draw the analogous conclusion that stabilization of ROP monomers by low GdnHCl concentration and unfolding by high concentration need not necessarily be a contradiction. Rather it is a manifestation of the complex action of chemical denaturants that may require a more elaborate description than simple binding equilibria. We shall pursue these ideas in the future to accomplish a quantitative description of the phenomenon.

Stability of Native ROP Results Predominantly from Interhelical Interactions in the Dimer. The four-α-helix-bundle structure of ROP is practically all α-helical, if one accounts for the apparent decrease in the percentage of α-helicity by the mobile C-terminal residues. It is characteristic of this structural motif that intersubunit interactions resulting from interdigitation between apolar residues on neighboring helices appear to play the decisive role in the stabilization of tertiary structure. This conclusion is strongly supported by the absence of stable monomers under native conditions in the unfolding equilibria. A similar situation has occurred with the dimeric Arc-repressor protein studied by Bowie and Sauer (1989). To get an estimate of the extent to which stability of the four-α-helix-bundle structure of ROP results from intrinsic α-helix stability of the two monomers or from interhelical interactions in the dimer, we performed isothermal GdnHCl unfolding studies as well as temperature-induced CD and heat capacity measurements in the presence of the denaturant.

The drop in the molecular weight between 35 and 50 °C and the independence of T_m = 51.2 °C on protein concentration in the presence of 2.5 M GdnHCl prove the existence of monomers having native-like secondary structure on the basis of their mean residue ellipticity. At low temperature (19 °C)

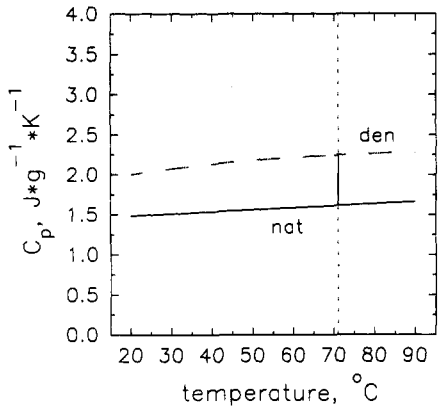

FIGURE 11: Dependence on temperature of the specific heat capacity of the native and unfolded states of ROP protein. The curve for the native state is the predenaturational heat capacity function as obtained from the DSC studies. It has been extrapolated into the transition region by using the equation $C_p^N(t) = (2.520 \times 10^{-3})t + 1.435$ (in J·g^{-1}·K^{-1}). The specific heat capacity function of the unfolded state has been calculated using the parameters given in Makhatadze and Privalov (1990). The equation is $C_p^D(t) = (2.297 \times 10^{-7})t^3 - (8.479 \times 10^{-5})t^2 + (1.090 \times 10^{-2})t + 1.818$ (in J·g^{-1}·K^{-1}). The dashed vertical line indicates the heat capacity difference at $t = T_m = 71$ °C of $\Delta C_p(T_m) = C_p^D(T_m) - C_p^N(T_m) = 0.633$ J·g^{-1}·K^{-1} = 9.1 kJ·(mol of dimer)$^{-1}$·K^{-1}.

breakdown of the dimeric structure starts only at about 4 M GdnHCl, as the sedimentation equilibrium studies show. Analysis of the isothermal unfolding curves, such as given in Figure 7b, on the basis of a simple N ⇔ D mechanism yields, by extrapolation to 0 M GdnHCl, the Gibbs energy of unfolding of the monomer. The corresponding numerical value is $\Delta G_D° = 22.4$ kJ·(mol of monomer)$^{-1}$. If we compare twice this value with the Gibbs energy change obtained from the DSC studies in the absence of the denaturant, we obtain an estimate for the contribution from helix–helix packing. The results shows that approximately 38% of the overall stability of ROP originates from the specific packing in the four-α-helix-bundle structure.

Perturbation of interhelix interactions in the dimer by GdnHCl was also used to get an estimate of the interaction enthalpy of the monomers. Monomerization of ROP should manifest itself not only in a decrease in conformational stability but also in a drastic reduction of the enthalpic interactions. Therefore the simultaneous cooperative decrease of transition enthalpy and transition temperature in the concentration range 0.5–2.5 M GdnHCl (Figure 9) must be attributed to the breakdown of the four-helix-bundle structure into monomeric species. The enthalpy difference of about 320 kJ·(mol of dimer)$^{-1}$ between native dimeric ROP and monomeric ROP in 2.5 M GdnHCl solution is an approximate measure of the interhelical forces that contribute to the overall transition enthalpy.

Experimental Heat Capacity Changes of ROP in the Presence of GdnHCl Are in Good Agreement with Estimates from Group Parameters. Using Hess's law we can obtain from the curves in Figure 9a,b a rough idea about the apparent heat capacity change involved in the disruption of the four-α-helix-bundle structure. At 71 °C ROP unfolds with the absorption of 580 kJ·(mol of dimer)$^{-1}$; in the presence of 2.5 M GdnHCl the values decrease to 51.6 °C and 260 kJ·(mol of dimer)$^{-1}$, respectively. The apparent heat capacity change is 15.9 kJ·(mol of dimer)$^{-1}$·K^{-1}. As expected it is considerably larger than the ΔC_p of unfolding observed in the absence of GdnHCl (10.3 kJ·(mol of dimer)$^{-1}$·K^{-1}), since the value contains the solvation contribution from the interaction with GdnHCl of the amino acid residues that become accessible on opening of the hydrophobic core of ROP. Recent careful studies by Makhatadze and Privalov (1992) resulted in parameters that permit an estimate of the additional heat capacity change observed in protein unfolding in the presence of GdnHCl. Our data are in qualitative agreement with the parameters given by these authors in that we observe a considerably larger ΔC_p^{app} in the presence of GdnHCl. The quantitative comparison is, however, difficult, because solvation contributions are of course dependent on the sequence and structure of the protein. Using Makhatadze's average parameter for ribonuclease (0.3 J·g^{-1}·K^{-1}), one computes for ROP a heat capacity change of 4.3 kJ·(mol of dimer)$^{1-}$·K^{-1} in excess to that observed in the absence of GdnHCl [ΔC_p = 10.3 kJ·(mol of dimer)$^{-1}$·K^{-1}]. It may well be possible that the unusually large number of hydrophobic residues that are exposed on unfolding the four-helix-bundle structure of ROP contribute to the relatively large ΔC_p change in general and the extra solvation contribution in the presence of GdnHCl.

We calculated also the ΔC_p value of ROP in the absence of GdnHCl from group parameters. We determined the coefficients for the heat capacity polynomial of the denatured state of ROP from the amino acid parameters given by Makhatadze and Privalov (1990) and used the experimental predenaturational linear heat capacity function to extrapolate the heat capacity of the native state to the transition temperature. The results of these calculations are shown in Figure 11 as specific heat capacity functions of the denatured (upper curve, dashed line) and the native state (lower curve, solid line). The specific heat capacity difference at T_m, Δc_p, is shown as a bar connecting the curves at T_m. The molar value, ΔC_p, between these functions at $T_m = 71$ °C is 9.05 kJ·(mol of dimer)$^{-1}$·K^{-1}. This ΔC_p estimate is smaller by about 12% than the experimental ΔC_p. In view of the difficulties involved in determining precise ΔC_p values in experiment and theory, the agreement between the calculated and measured ΔC_p values is excellent.

REFERENCES

Almassy, R. J., & Dickerson, R. E. (1978) *Proc. Natl. Acad. Sci. U.S.A. 75*, 2674–2678.

Arakawa, T., Bhat, R., & Timasheff, S. N. (1990) *Biochemistry 29*, 1914–1923.

Banner, D. W., Kokkinidis, M., & Tsernoglou, D. (1987) *J. Mol. Biol. 196*, 657–675.

Bellelli, A., Ippoliti, R., Brancaccio, A., Lendaro, E., & Brunori, M. (1990) *J. Mol. Biol. 213*, 571–574.

Bowie, J. U., & Sauer, R. T. (1989) *Biochemistry 28*, 7139–7143.

Brandts, J. F., & Lin, L. N. (1990) *Biochemistry 29*, 6927–6940.

Casassa, E. F., & Eisenberg, H. (1964) *Adv. Protein Chem. 19*, 287–395.

Castagnoli, L., Scarpa, M., Kokkinidis, M., Banner, D. W., Tsernoglou, D., & Cesareni, G. (1989) *EMBO J. 8*, 621–629.

Cesareni, G., Helmer-Citterich, M., & Castagnoli, L. (1991) *Trends Genet. 7*, 230–235.

Cesareni, M., Muesing, M. A., & Polisky, B. (1982) *Proc. Natl. Acad. Sci. U.S.A. 79*, 6313–6317.

Cohen, C., & Parry, D. A. D. (1986) *Trends Biochem. Sci. 11*, 245–248.

Cohen, C., & Parry, D. A. D. (1990) *Proteins: Struct., Funct., Genet. 7*, 1–15.

Cohn, E., & Edsall, J. T. (1943) in *Proteins, Amino Acids, and Peptides*, pp 155–176 and 370–381, Reinhold Publishing Corp., New York.

Crick, F. H. C. (1953) *Acta Crystallogr. 6*, 689–697.

Eberle, W., Klaus, W., Cesareni, G., Sander, C., & Roesch, P. (1990) *Biochemistry 29*, 7402–7407.
Flossdorf, J. (1980) *Makromol. Chem. 181*, 3228–3232.
Flossdorf, J., & Schillig, H. (1979) *F&M, Feinwerktech. Messtech. 87*, 93–96.
Hinz, H.-J. (1979) in *Biochemical Thermodynamics* (Jones, M. N., Ed.) pp 116–167, Elsevier Scientific Publishing Co., London.
Ho, S. P., & DeGrado, W. F. (1987) *J. Am. Chem. Soc. 109*, 6751–6758.
Huber, R. (1988) *Angew. Chem. 100*, 79–89.
Jaenicke, R. (1991) *Eur. J. Biochem. 202*, 715–728.
Kawahara, K., & Tanford, C. (1966) *J. Biol. Chem. 241*, 3228–3232.
Kiefhaber, T., Schmid, F. X., Renner, M., Hinz, H.-J., Hahn, U., & Quaas, R. (1990) *Biochemistry 29*, 8250–8257.
Lacatena, R. M., Banner, D. W., Castagnoli, L., & Cesareni, G. (1984) *Cell 37*, 1009–1014.
Makhatadze, G. I., & Privalov, P. L. (1990) *J. Mol. Biol. 213*, 375–384.
Makhatadze, G. I., & Privalov, P. L. (1992) *J. Mol. Biol. 226*, 491–505.
Marky, L. A., & Breslauer, K. J. (1987) *Biopolymers 26*, 1601–1620.
Nojima, H., Hon-nami, K., Oshima, T., & Noda, H. (1978) *J. Mol. Biol. 122*, 33–42.
Nozaki, Y. (1972) *Methods Enzymol. 26*, 43–50.
Perkins, S. J. (1986) *Eur. J. Biochem. 157*, 169–180.
Privalov, P. L. (1979) *Adv. Protein Chem. 33*, 167–241.
Privalov, P. L., Plotnikov, V. V., & Filimonov, V. V. (1975) *J. Chem. Thermodyn. 7*, 41–47.
Renner, R., Hinz, H.-J., Scharf, M., & Engels, J. W. (1992) *J. Mol. Biol. 223*, 769–779.
Sanbongi, Y., Igarashi, Y., & Kodama, T. (1989) *Biochemistry 28*, 9574–9578.
Schellman, J. A. (1990) *Biophys. Chem. 37*, 121–140.
Schmid, F. X. (1989) in *Protein structure—a practical approach* (Creighton, T. E., Ed.) pp 251–285, IRL Press, Oxford.
Timasheff, S. N. (1992) *Biochemistry 31*, 9857–9864.
Tomizawa, J.-I. (1990) *J. Mol. Biol. 212*, 695–708.
Tomizawa, J.-I., & Som, I. (1984) *Cell 38*, 871–878.
Twigg, A. J., & Sherrat, D. (1980) *Nature 283*, 216–218.
Weber, P. C., & Salemme, F. R. (1980) *Nature 287*, 82–84.
Yang, J.-T., Wu, C.-S. C., & Martinez, H. M. (1986) *Methods Enzymol. 130*, 208–269.